Evidence for a metastable state of the fundamental dianion H^{2-}

T. Sommerfeld, U. V. Riss, H.-D. Meyer, and L. S. Cederbaum
Theoretische Chemie, Physikalisch-Chemisches Institut, Universität Heidelberg, Im Neuenheimer Feld 253, 69120 Heidelberg, Germany
(Received 7 November 1996)

A resonance state with three equivalent electrons and one proton has been identified. Large-scale calculations have been performed using the complex-rotation technique, and the results indicate that the investigated $^4S^o$ state of H^{2-} is strongly correlated. The findings are rationalized by comparing with bound doubly charged anions, isoelectronic states of the Li atom, and calculations in the infinite-dimension limit. In addition, the emerging picture is sustained by an analysis of the complex-rotated wave function. [S1050-2947(97)06803-0]

PACS number(s): 31.25.−v, 32.70.Fw, 32.80.Dz

I. INTRODUCTION

After an interval of 15 years, we have seen a revival of interest in the prototype dianion H^{2-}. Results obtained in the early 1970s have been questioned and demonstrated to be flawed, and new questions have emerged from noval contexts. Let us briefly outline these two phases of H^{2-} investigations and shed light on the different perspectives on this fundamental system.

On the one hand, the H^{2-} system was studied from an electron scattering point of view. The collision process $e+H^- \rightarrow H+e+e$ was examined and the observation of two pronounced structures in the cross section was interpreted as the formation of two metastable H^{2-} states [1–3]. The experimental findings were supported by stabilization calculations, which determined two $^2P^o$ resonance states at roughly the energies observed [4,5]. However, the resonances were detected at energies slightly above the threshold for complete breakup of the system into a proton and three free electrons and therefore contradict Simon's theorem [6,7]. Simon showed that in any many-particle system experiencing only Coulombic forces, resonances cannot exist above the threshold for complete disintegration of the system. The existence of metastable $^2P^o$ H^{2-} states was first questioned in 1977 [8,9] and almost 20 years later, in 1994, the results of Refs. [4] and [5] were shown to be most probably artifacts of a too small basis set [7]. Furthermore, in a new, high-resolution measurement of the electron-H^- scattering cross section no structure related to the existence of short-lived H^{2-} states was observed [10,11]. One may conclude that there are no H^{2-} resonances above the triple-escape threshold and that there are in fact no indications for metastable doublet states of H^{2-}.

On the other hand, H^{2-} was investigated from a ''bound-state'' perspective, emphasizing the possible existence of H^{2-} states stable or metastable with respect to autodetachment. Contemporarily with the first e-H^- scattering experiments it was proved that a proton cannot permanently bind three electrons [12], a theorem that later was generalized by Lieb [13]. Furthermore, in 1978 two independent high-quality *ab inito* investigations showed that H^{2-} possesses no excited bound state, i.e., no state that is bound with respect to the correspondingly excited H^- ion and a free election [14,15]. Thus, if there is any metastable state of H^{2-}, it has to be a shape or core excited shape resonance, which typically show lifetimes in the range of 10^{-14}–10^{-16} s.

Recently, the latter perspective has attracted considerable attention in the context of free molecular dianions. Only recent experimental and theoretical studies have definitely shown that in spite of the large Coulomb repulsion small dianions may exist as isolated entities. The fundamental question, ''which is the smallest molecular or atomic system that can bind two excess electrons?'' and the properties that allow small molecular species to form stable dianions have drawn substantial interest [16,17]. From this more global point of view a metastable state of H^{2-} is especially attractive, since it may contribute to a principal understanding of these delicate systems. Previously [18] we have presented evidence that such a state does indeed exist and rationalized its structure by comparison with molecular dianions and calculations in the large dimension limit. In the present communication we will describe the theoretical techniques employed in far more detail and discuss our numerical results (Secs. II and III). In Sec. IV we will analyze the electronic structure of the metastable H^{2-} state and compare it with the corresponding bound state of He^-. Section V constitutes a summary.

II. TECHNICAL DETAILS

In the first part of this section we would like to survey the complex-rotation (CR) method [19–24], which has been employed to calculate the energy and the lifetime of the investigated resonance state. In the second part we will describe the specific numerical approach in more detail. In the CR method the set of electronic coordinates $\{r\}$ of the Hamiltonian is simultaneously rotated into the complex plane, that is, $\hat{H}(\{r\}) \rightarrow \hat{H}(\{e^{i\theta}r\}) \equiv \hat{H}(\theta)$. Note that in contrast to $\hat{H}$ the rotated Hamiltonian $\hat{H}(\theta)$ is complex symmetric and *not* Hermitian. Despite that, the bound states remain unchanged, i.e., the bound states of $\hat{H}(\theta)$ have the same (real) energies as those of $\hat{H}$. However, the energies of the unbound states are rotated into the complex energy plane. The continuum states of $\hat{H}(\theta)$ lie on rays, where each ray is associated with a scattering threshold and makes an angle of -2θ with the real energy axis. If resonance states have been uncovered by the rotation of the continuum rays, they appear with discrete complex eigenvalues

$$E_{\mathrm{res}} = E - i\Gamma/2, \tag{2.1}$$

where E is the position and $1/\Gamma$ is the lifetime of the resonance. Furthermore, the wave functions corresponding to uncovered resonance states vanish as any of the electronic coordinates tends to infinity, such that the resonance state as well as the bound states can be represented by square integrable (L^2) functions. Thus, the complex rotation allows us to treat resonance states on the same footing as bound states, both can be expanded in a standard L^2 basis set, and the available vast quantum chemical technology may be applied.

The price one has to pay for the L^2 description of a resonance wave function lies primarily in the loss of hermiticity, associated to the complex energies of resonance states. It is necessary to introduce a bilinear form, the c product:

$$(\Psi|\Phi) \equiv \int \Psi\Phi\, d\tau, \tag{2.2}$$

where in contrast to the Hermitian product $\langle\Psi|\Phi\rangle$ the left-hand function Ψ is *not* taken to be complex conjugated in the integral [25]. The eigenvectors of $\hat{H}(\theta)$ are then c normalizable, and in a practical calculation one has to work with complex vectors. There are a number of further drawbacks in the CR technique related to the oscillatory behavior of core orbitals introduced by the rotation and the application to molecular systems (see, e.g., the discussion in [26]), but these do not apply to the H^{2-} state investigated in the present context.

For an atomic system the CR technique may be applied in a straightforward manner, since $e^{-i\theta}$ simply factors out the Coulomb potentials. If **T** and **V** are the real-valued matrices of the kinetic and potential energies, e.g., in an atomic configuration-interaction (CI) calculation, the complex symmetric matrix of the rotated Hamiltonian $\hat{H}(\theta)$ is given by

$$\mathbf{H}(\theta) = e^{-2i\theta}\mathbf{T} + e^{-i\theta}\mathbf{V}. \tag{2.3}$$

Instead of working directly with $\mathbf{H}(\theta)$ it is advantageous to diagonalize the matrix

$$e^{i\theta}\mathbf{H}(\theta) = \mathbf{H} + (e^{-i\theta} - 1)\mathbf{T}, \tag{2.4}$$

where $\mathbf{H} = \mathbf{T} + \mathbf{V}$ is the unrotated Hamilton matrix. In this way only the one-particle matrix **T**, which is extremely sparse in comparison to **V** or **H**, has to be multiplied by a complex factor depending on the rotation angle. Thus, the matrix times vector operation, which is the bottleneck in any iterative diagonalization procedure, can be separated into two steps. The first, and time-consuming, step is the multiplication with the real-valued matrix **H** and only the second step, the multiplication with $(e^{-i\theta} - 1)\mathbf{T}$, involves complex matrix elements. Finally, the obtained eigenvalues are multiplied with $e^{-i\theta}$ to obtain the eigenvalues of $\mathbf{H}(\theta)$.

We now turn to the description of the specific one- and many-particle basis sets we employed in our calculations. In the H^{2-} system electron correlation may be expected to be extremely important. Thus, we used the multireference configuration-interaction approach (MR-CI) to construct the three-particle basis functions for the complex rotated Hamiltonian $\hat{H}(\theta)$. The underlying one-particle basis sets were built of uncontracted Cartesian Gauss-type orbitals (GTO). In the following the values for the GTO exponents are given for $Z = 1$; for other values of Z the exponents have been scaled with Z^2. The smallest basis set comprises 18 even scaled p-type functions, where the largest exponent is 1.0, the scaling factor is 1.6, and consequently the smallest exponent is 0.00034. Larger basis sets were constructed by adding seven s-type and up to five even scaled d-type functions beginning with an exponent of 0.05 and a scaling factor of 2.0. The largest basis set includes two additional f-type functions with exponents of 0.03 and 0.01. The seven s-type functions stem from the atomic natural orbital basis set in the MOLCAS program [36] (plus one diffuse function) and were added to perform self-consistent field (SCF) and complete active space self-consistent field (CASSCF) calculations prior to the MR-CI procedure. The corresponding orbitals were used to build the three-particle basis functions and will be discussed further below.

The energy of the highly correlated ${}^3P^e$ state of H^- provides a useful criterion to check the quality of our GTO basis sets, since the full configuration-interation result is readily obtained. Employing the $7s18p5d$ basis this energy is -0.12525 a.u., only 50×10^{-6} Hartree above the result from [14] ($6p4d$ Slater-type orbitals basis set with state-specific optimized exponents), and 100×10^{-6} Hartree above Drake's presumably exact result [27]. Another check for the basis set is provided by a second nonlinear scaling parameter α. Instead of using $e^{i\theta}$ one scales the electronic coordinates with $\alpha e^{i\theta}$ [25] and in a calculation employing a finite basis set both parameters θ and α have to be optimized (see discussion in the next section). The parameter α effectively scales the exponents of the basis set and the computed α trajectories show that our results depend only very weakly on α (with $\alpha_{\mathrm{opt}} \approx 1.0$). Thus, our one-particle basis set performs satisfactorily.

The three-particle configuration space for the $(2p^3)^4S^o$ state was then generated by all single and double excitations relative to a set of 18 (np^3)-type reference configurations. By this means a full-CI (FCI) expansion within the p-orbital space is obtained and all excitations of one or two electrons into the s, d, or f orbitals are taken into account. Since we are using FCI or nearly FCI expansions for the $18p$ or larger basis sets, respectively, in principle the underlying one-particle orbitals used to construct the configuration space should be irrelevant. However, the band Lanczos diagonalization of the Hamilton matrix is an iterative procedure and the convergence of this iteration does depend on the space spanned by the start vectors. In our calculations the start vectors were the 18 Cartesian vectors representing the 18 reference configurations, and thus, the choice of orbitals has a major influence on the iteration. Several sets of self-consistent field (SCF) orbitals have been used and two sets turned out to yield a far better convergence in the Lanczos procedure than any other we tried. These were, on the one hand, the SCF orbitals of H ($1s^1$), and on the other hand, orbitals originating from a CASSCF calculation for the ${}^4S^o$ state of He^- (three electrons in nine active orbitals).

The MOLCAS package of programs [36] has been used for the SCF and CASSCF calculations, and the MRDCI program of Engels, Pless, and Suter [28] has been employed to compute the matrix **H**. Subsequently, the matrix $(e^{-i\theta} - 1)\mathbf{T}$ has

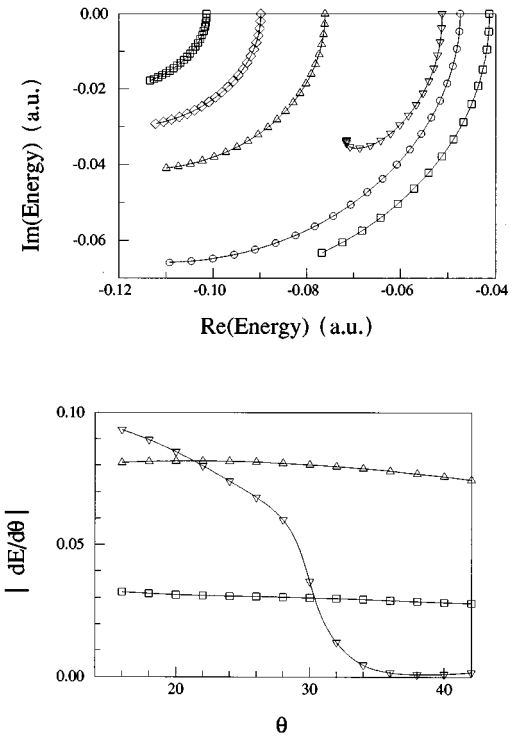

FIG. 1. In the upper panel the eigenvalue trajectories of the resonance and five typical other states in the complex energy plane are shown for rotation angles $0° \leqslant \theta \leqslant 42°$ in steps of 2°. In the lower panel the corresponding velocities of the trajectories of the first and third continuum and of the resonance state are displayed. The $7s18p5d$ basis set has been used.

been constructed and the spectrum of $e^{i\theta}\mathbf{H}(\theta)$ has been computed with a band-Lanczos program adapted to the case of complex symmetric matrices [29–31].

III. NUMERICAL RESULTS

Before we study the energy and lifetime of the $(2p^3)^4S^o$ state, let us briefly discuss the consequences of expanding $\hat{H}(\theta)$ in a finite basis. Using a complete, infinite basis set the complex resonances energy $E_{\rm res}$ is independent of the rotation angle θ once it has been uncovered. However, this is not the case if finite basis sets are employed. In practical CR calculations it has been observed that if the rotation angle θ is increased the resonance eigenvalue rotates towards the resonance position, slows down, and then moves rapidly away. In other words, the resonance energy $E_{\rm res}$ is a function of θ, but shows stationary behavior near a particular value $\theta_{\rm opt}$. Clearly, for this value of θ the given finite basis set describes the resonance state in an optimal way and the associated $E_{\rm res}$ is the best value for the resonance energy. Thus, one has to compute the complex spectrum of $\hat{H}(\theta)$ for several rotation angles and to investigate the trajectories of the eigenvalues. As an example in Fig. 1 the θ trajectories of the $^4S^o$ H^{2-} resonance state and five typical other states are shown in the range $0° \leqslant \theta \leqslant 42°$ with steps of 2°. The resonance eigenvalue shows a pronounced stability for $\theta \geqslant 30°$ (the corresponding seven $E_{\rm res}$ values can hardly be distinguished on the energy scales of Fig. 1) whereas the typical

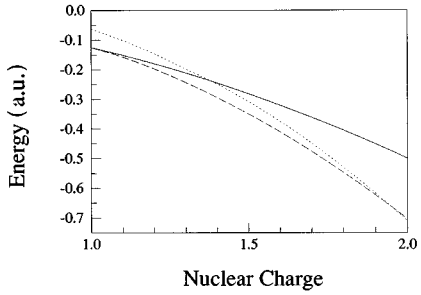

FIG. 2. Total energy of three different electronic states discussed in the text. Continuous line: one-electron $(2p^1)^2P^o$ state; dashed line: two-electron $(2p^2)^3P^e$ state; dotted line, three-electron $(2p^3)^4S^o$ state. For the latter state the real part of the complex energy is shown.

continuum eigenvalues rotate with θ. This behavior becomes even more evident if the velocities $|dE/d\theta|$ of the different trajectories are considered. Whereas typical continuum eigenvalues show a ''constant'' velocity, the velocity of the resonance eigenvalue decreases dramatically when $\theta_{\rm opt}$ is approached (Fig. 1). The influence of the basis set on this stabilization behavior of the resonance eigenvalue will be discussed later.

In the remainder of this section we will regard the energies (and lifetimes) of the three states $(2p^1)^2P^o$, $(2p^2)^3P^e$, and $(2p^3)^4S^o$ as functions of the nuclear charge Z and, in particular, discuss the development of these states when the nuclear charge is decreased from $Z=2$ (He-He^-) to $Z=1$ (H^--H^{2-}). For $Z=2$ the $(2p^2)^3P^e$ He state is much lower in energy than the corresponding $^2P^e$ He^+ cation. In contrast, for $Z=1$ it has been shown that the $^3P^e$ state of H^- is just 0.00035 a.u. [27] below the $^2P^o$ state of H. These changes of energy involved in proceeding from $Z=2$ to $Z=1$ have been displayed in Fig. 2. The continuous line represents the energy of the $(2p^1)^2P^o$ state, which simply equals $-Z^2/8$, and the dashed line shows the energy of the $(2p^2)^3P^e$ state obtained at the FCI level of theory using the $18p$ basis set. Clearly, the two energies approach each other, and for $Z=1$ they become virtually equal.

The energy of the three electron $(2p^3)^4S^o$ state is represented by the dotted curve. This state is bound with respect to electron loss for He^-, but clearly unbound for H^{2-} [15]. Consequently, in going from $Z=2$ to $Z=1$ its energy has to cross the energies of the two former states and turn into a resonance. For those values of Z, where the $^4S^o$ state is unstable to autodetachment, the real part of its energy is shown. As can be seen in Fig. 2, the crossing with the two-electron $^3P^e$ state occurs very close to He. If the nuclear charge is decreased from its initial value of 2 the $^4S^o$ state becomes rapidly unstable with respect to electron loss and moves into the $(2p^2\epsilon p)$ continuum. At $Z \approx 1.4$ the channel to the $(2p^1\epsilon p\epsilon' p)$ continuum opens; i.e., the $(2p^3)$ $^4S^o$ state becomes unstable with respect to the loss of two electrons. Nevertheless, for $Z=1$ the $^4S^o$ resonance state still shows a negative energy of -0.063 a.u. (FCI-$18p$); i.e., the system is stable with respect to complete breakup into the nucleus and three free electrons. Simon's theorem is therefore not violated. Using larger basis sets that contain functions of higher angular momentum the resonance position for $Z=1$ is even decreased to -0.071 a.u. (MR-CI–$7s18p5d$)

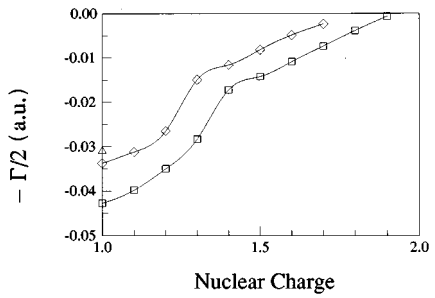

FIG. 3. The imaginary part of the complex energy of the $(2p^3)^4S^o$ state is shown. The curves give the results for different basis sets. Squares: $18p$ basis; diamonds: $7s18p5d$ basis; triangle: $7s18p5d2f$ basis.

and -0.072 a.u. (MR-CI–$7s18p5d2f$), respectively, i.e., larger basis sets stabilize the H^{2-} resonance state.

We now turn to the associated lifetime of the $(2p^3)$ $^4S^o$ state. Our results for the imaginary part of the resonance energy are shown in Fig. 3. At first glance, surprisingly, the resonance width, in contrast to the resonance position, is not a smooth function of Z. However, ''cusps'' in the lifetime are to be expected, whenever a new channel opens. We attribute the cusps in our curves between $Z=1.4$ and $Z=1.3$ to the opening of the $(2p^1\epsilon p\epsilon' p)$ two-particle breakup channel. Furthermore, we observe again that in going from the $18p$ to a larger basis set the $^4S^o$ resonance state is stabilized. Firstly, for a particular value of Z the resonance width is reduced, if functions of higher angular momentum are added to the basis set. For example, for $Z=1$ the width falls from 0.043 a.u. for the $18p$ basis to 0.034 a.u. for the $7s18p5d$ and 0.032 a.u. for the $7s18p5d2f$ basis set. Secondly, the cusp in the curve displaying the resonance width is shifted by about 0.1 a.u. to lower Z, if the larger basis is used. This indicates a later crossing of the resonance Z trajectory with that of the $(2p^2)^3P^e$ state. Thus, if the basis set is enlarged, the stabilization of the $^4S^o$ resonance state is reflected in two respects. On the one hand, the resonance position is lowered, i.e., H^{2-} is stabilized with respect to the $^3P^e$ state of H^-, and, on the other hand, the lifetime of the $^4S^o$ H^{2-} state is increased. We conclude that both a larger one-particle basis set including basis functions of even higher angular momentum and a larger MR-CI space will tend to stabilize further the H^{2-} resonance state.

Let us briefly comment on the dependency of our results on the number of d-type polarization functions in the basis set. Whereas the real part of the complex energy needs about four additional d-type functions to converge, the lifetime values depend only weakly on the particular number of d- or f-type functions. One function seems to be sufficient provided that the corresponding exponent has an appropriate value. However, if four or five d-type functions are used, the stationary behavior of the θ trajectory of the resonance state is far more pronounced. Clearly, the polarization basis set has to provide a certain flexibility to describe the resonance wave function over an appreciable θ range. Consequently, it yields a greater stability of the complex eigenvalue with respect to the rotation angle.

As our final result we predict the existence of a $(2p^3)^4S^o$ resonance state of H^{2-} with a resonance position of about 1.4 eV above the $(2p^2)^3P^e$ state of H^- (i.e., 12.4 eV above the $^1S^e$ ground state of H^-) and a width of 1.7 eV corresponding to a lifetime of 3.8×10^{-16} s. Note, however, that the $^4S^o$ state would not be seen in electron scattering from the $^1S^e$ ground state of H^-.

IV. DISCUSSION

Having established a $^4S^o$ resonance state of the H^{2-} dianion, this section is concerned with the interpretation of our findings. In a previous communication we have suggested rationalizing the stability of the H^{2-} system in terms of an increased average angle between the electrons [18]. This picture is based on the analogy to molecular dianions of the $AX_3{}^{2-}$ type, where A is an alkali metal and X is fluorine or chlorine. Here we briefly repeat our argument. The $AX_3{}^{2-}$ dianions may be thought of as three X^- anions bound to a A^+ cation [32], i.e., to consist of one positively and three negatively charged particles. In this way they resemble the H^{2-} system, but, in contrast to H^{2-}, the short-range part of the potential is dominated by the Born repulsion of the atomic cores. The $AX_3{}^{2-}$ species themselves are stable with respect to electron autodetachment and show a very broad barrier to loss of an X^- ion. Thus, they represent a long-lived resonance state of the four-particle system $A^+(X^-)_3$ and the local stability of the composite system can be rationalized in electrostatic terms: in the vicinity of the D_{3h} equilibrium geometry the Coulombic attraction between the central A^+ cation and the X^- ligands overcompensates the Coulomb repulsion between the three X^- ions and a stable dianion is formed. An analogous effect may be conceivable for the $^4S^o$ H^{2-} state, if the electronic motion is correlated is such a way as to maintain an approximately triangular configuration around the nucleus.

In [18] we presented further evidence for this interpretation. On the one hand, we analyzed the electron-nucleus-electron angle φ of a three-electron atom in the large dimension limit, where the electrons occupy fixed positions in space. For large nuclear charges Z the angle φ is found to be close to 90°, but, if Z is decreased the system gets more diffuse and φ grows to about 103° for $Z=1$. On the other hand, a series of (np^3) $^4S^o$ states of the Li atoms has been studied in the literature [33,34]. For $n=2$ an interelectronic angle of 90° was found, and this angle tends to 120° in the limit of $n\rightarrow\infty$. Thus, in both cases the same trend was observed. The compact systems ($Z\gg1$, $n=2$) show electron-nucleus-electron angles close to 90°, and the more diffuse the system gets, if n in increased or Z is decreased, respectively, the further this angle is enlarged. Thus, a situation in analogy to the $AX_3{}^{2-}$ dianions is approached, and the picture derived from this molecular system is indeed sustained.

In the remainder of this section we will examine the electrostatic interpretation more directly by investigating the complex wave function of the resonance state. When we began this study, we have computed the CI wave functions of the $^4S^o$ states of H^{2-} and He^-, but it was by no means clear how to extract the relevant information. This wave function is a complicated, nine-dimensional function, and in order to draw conclusions one has to reduce this complexity without losing the important information to averaging. Usually, a CI vector can be analyzed by directly inspecting its dominant

components. However, here the CI vector contains a very large number of $(np_x n' p_y n'' p_z)$ configurations of approximately equal weights. These configurations reveal nothing about the angular correlation, since a basis set consisting of p-type functions only yields an average interelectronic angle of 90° (see below). Even a closer examination of the d contributions does not provide any readily comprehensible information. Eventually, we decided to calculate overlaps with model functions of three and two electrons, respectively. Loosely speaking, we were raising the questions ''how large is the contribution of a certain geometrical configuration of the electrons to the wave function?'' and ''what is the third electron doing if we fix the position of the other two?'' In the following paragraphs we will describe these model functions used to interpret the CI wave function and discuss the results.

Let us begin with the former question. We intend to describe a geometrical configuration of three equivalent electrons that have an equal distance R from the nucleus and a fixed electron-nucleus-electron angle ϕ, i.e., describing a geometrical situation analogous to the ammonia molecule. A corresponding three-electron model function $\Psi^{(3)}(R,\phi)$ was constructed as the antisymmetric product of three off-center s-type GTO's,

$$\Psi^{(3)} = N\mathcal{A}(\chi_1\chi_2\chi_3), \quad \chi_i(\vec{r}_i) = \exp[-\alpha(\vec{R}_i - \vec{r}_i)^2], \tag{4.1}$$

where N is a normalization constant, $\mathcal{A}$ is the antisymmetrizing operator, and $|\vec{R}_i| = R$. The set $\{\vec{R}_i\}$ was chosen in accord with C_{3v} symmetry for $\phi < 120°$, and for the limiting angle $\phi = 120°$ the system is planar and the symmetry is D_{3h}. The larger the exponent α is chosen, the more strongly localized are the three electrons described by $\Psi^{(3)}$. However, α cannot be chosen arbitrarily large, since the GTO's χ_i have to be expressed in our finite nucleus-centered basis set. In our calculations a value of $\alpha = 10$ a.u. turned out to yield reasonable results and the data presented in the following have been obtained using this value. For $\alpha = 10$ our basis set is still capable to represent the χ_i. The overlap of our model function $\Psi^{(3)}$ with the CI vector shows appreciable values only for $R \gg 1/\sqrt{\alpha}$. This overlap $(\Psi^{(3)}(R,\phi)|\Psi^{\mathrm{CI}}(\{\vec{r}_i\}))$ then represents the weight of the specific geometrical structure defined by R and ϕ and we can try to identify a ''dominant'' configuration.

At this point let us emphasize that we consider a complex-rotated wave function. The overlap with the real test function $\Psi^{(3)}$ thus depends on the complex-rotation angle θ. The complex-rotated wave function describes the resonant part of the wave function much clearer than the nonrotated one. The latter is dominated by the exponentially increasing asymptotic part describing the here irrelevant aspect of H^- plus a free electron. It is thus meaningful to investigate the complex-rotated wave function rather than the unrotated one (which is not available anyway). The angular distribution, which is our prime interest, depends very weakly on the complex-rotation angle θ as soon as the resonance is uncovered. The radial distribution may depend more strongly on the rotation angle θ but we even expect the radial distributions discussed below to be very meaningful, in particular their change upon enlargement of the basis set. To back up our arguments we applied this test function overlap procedure to the real and complex-rotated wave functions of the *bound* $(2p^2)^3P^e$ state of H^-. The absolute values of these overlaps turned out to be virtually independent of the rotation angle θ.

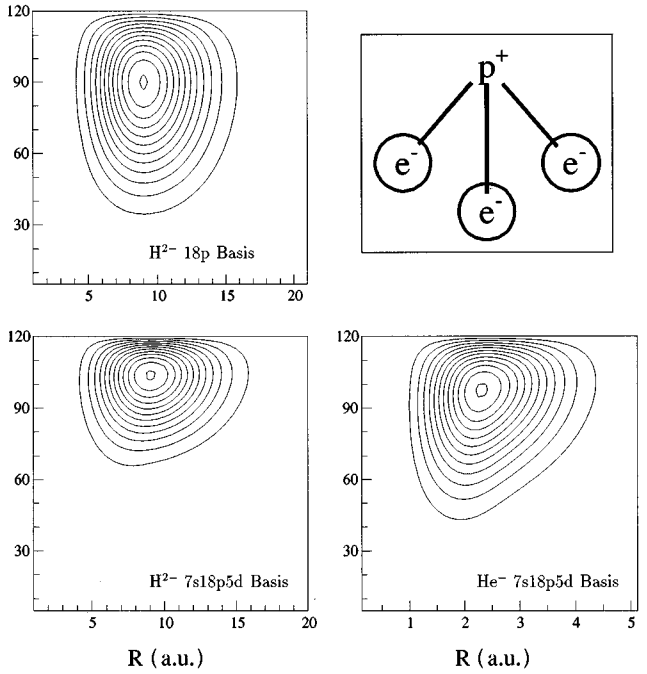

FIG. 4. Schematic representation of the model function $\Psi^{(3)}(R,\phi)$ and the associated values of the weighted overlap $W(R,\phi)$ (arbitrary units). The interelectronic angle ϕ is given in degrees, and the contour lines are evenly spaced, where the ratio between the innermost and outermost line is 11. Upper left: H^{2-} ($18p$ basis), lower left: H^{2-} ($7s18p5d$ basis), and lower right: He^- ($7s18p5d$ basis). Note the different scales on the R axis.

Let us return to the overlap of the CI vector with our model function $\Psi^{(3)}$. In Fig. 4 the weighted squared absolute value of the overlap W,

$$W(R,\phi) = R^3|(\Psi^{(3)}|\Psi^{\mathrm{CI}})^2|, \tag{4.2}$$

is shown for the $^4S^o$ states of H^{2-} ($18p$ and $7s18p5d$ basis) and He^- ($7s18p5d$ basis). The weight factor R^3 appearing in the equation above takes into account the total rotation (weight R^2) and internal rotation (weight R) of a given (R,ϕ) configuration. The distributions W of both systems H^{2-} and He^- look roughly the same. Both show a clear maximum and asymptotically tend to zero in all directions, resembling a slightly distorted Gaussian function. We note that this maximum of W in the (R,ϕ) space is a global maximum with respect to all nine coordinates $\{\vec{R}_i\}$ in $\Psi^{(3)}$. The angular distribution becomes more evident if W is integrated over R, providing a distribution function depending on the electronic angle ϕ only (Fig. 5). These functions of ϕ show again one well-defined maximum and exhibit widths of several 10°. Despite the appreciable widths, one may clearly think in terms of a certain geometrical configuration of the electrons, which depends on the nuclear charge and the flexibility of the basis set. In the following discussion we

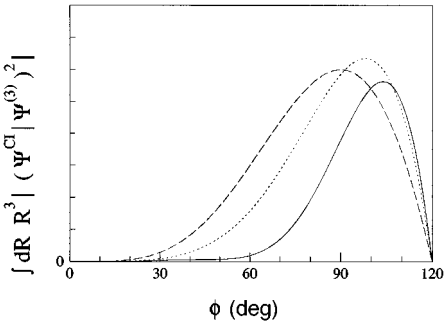

FIG. 5. Angular distribution for the overlap of the model function $\Psi^{(3)}$ with Ψ^{CI}. The weighted absolute value of the squared overlap $W(R,\phi)$ has been integrated over R. Continuous line: H^{2-}, $7s18p5d$ basis; dotted line: He^-, $7s18p5d$ basis; dashed line: H^{2-}, $18p$ basis.

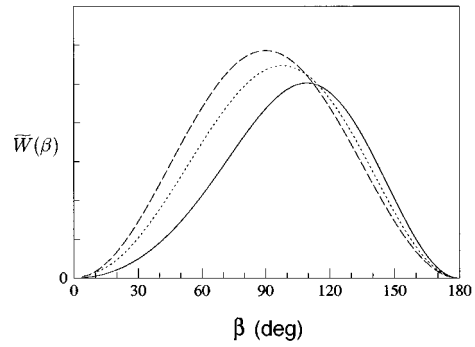

FIG. 6. The angular distribution $\widetilde{W}(\beta)$ defined in the text is shown. β is the angle in the two-particle model function, which is schematically displayed in Fig. 7. Continuous line: H^{2-}, $7s18p5d$ basis; dotted line: He^-, $7s18p5d$ basis, dashed line: H^{2-}, $18p$ basis.

will refer to the angle associated to the maximum of the integrated distribution W as the angle $\phi_{\max}$ between two electrons.

We first examine the basis set dependence of $\phi_{\max}$. For the $18p$ basis set $\phi_{\max}$ is found to have a value of 90° and the angular distribution is quite broad. If polarization functions are added to the basis set $\phi_{\max}$ is increased to about 104° for the $7s18p5d$ basis set and the associated width is strongly decreased. This trend is in accord with our interpretation of the energy and lifetime changes, which occur in going from the $18p$ to the $7s18p5d$ basis set [18]. A basis set consisting of p-type functions only forces an interelectronic angle of 90°, whereas polarization functions allow this angle to increase. By this means a situation closer to the D_{3h} symmetrical classical minimum of the $AX_3{}^{2-}$ system may be achieved, and the dianion is thus stabilized in two respects: its energy is decreased and its lifetime is increased.

Secondly, we consider the Z dependence of $\phi_{\max}$. Apart from the different R scales in Fig. 4 the distribution functions for H^{2-} and He^- ($7s18p5d$ basis) look very similar. These similarities in the overall shape of W emphasize that both systems are strongly related, regardless of the fact that one system is bound and the other is unstable to electron loss. In other words, the difference in Z essentially changes the length scale, but the overall characteristics of the electronic state are maintained. The differences that occur in proceeding from $Z=2$ to $Z=1$ are again more clearly seen in Fig. 5. For He^- $\phi_{\max}$ is about 5° smaller than for H^{2-} and the He^- angular distribution exhibits a larger width. Both trends reflect the decreased ratio between Coulomb repulsion and attraction for $Z=2$, and parallel the tendencies that have been observed in the limit of infinite dimension [18,35] and for highly exited $^4S^o$ states of Li [33,34]. As discussed above, the more diffuse the $^4S^o$-like systems become, the further increased is the associated interelectronic angle. Note, however, that for the atomic $^4S^o$ species the limiting angle of $\phi_{\max}=120°$ can only be approached but never be reached, since the symmetry of the $^4S^o$ state implies that $W(\phi\rightarrow 120°)\rightarrow 0$ (Figs. 4 and 5). The plane defined by the nucleus and any two electrons is a nodal plane for the third electron. We will shed light on this property in the context of the analysis using the two-electron model function $\Psi^{(2)}$ described in the following paragraphs.

We now turn to the latter question: ''What is the third electron doing if we fix the position of the other two?'' If the positions of two electrons $(\vec{R}_1,\vec{R}_2)$ are fixed, the probability amplitude to find the third electron is calculated by multiplying $\Psi^{\mathrm{CI}}(\vec{r}_1,\vec{r}_2,\vec{r}_3)$ with $\delta(\vec{R}_1-\vec{r}_1)\,\delta(\vec{R}_2-\vec{r}_2)$ and integrating over $\vec{r}_1$ and $\vec{r}_2$. However, since we work with a finite, nuclear-centered GTO basis set, which represents off-center δ functions very poorly, we represent the localized electrons again by relatively tight s-type GTO's,

$$\chi_i(\vec{r}_i)=\exp[-\alpha(\vec{R}_i-\vec{r}_i)^2] \tag{4.3}$$

at the positions $\vec{R}_1$ and $\vec{R}_2$. The qualitative conclusions are again independent of α as long as $1/\sqrt{\alpha}$ is smaller than all relevant distances. If the resulting one-particle function $\Psi^{(1)}(\vec{r})$ is expanded in the given basis set $\{\psi_i\}$ (e.g., the $7s18p5d$ basis)

$$\Psi^{(1)}(\vec{r})=(N\mathcal{A}(\chi_i\chi_2)|\Psi^{\mathrm{CI}})\equiv\sum\ c_i\psi_i\,, \tag{4.4}$$

the coefficients c_i are given as the overlap of the resonance wave function Ψ^{CI} and the single Slater determinant $N\mathcal{A}(\chi_i\chi_2\psi_i)$

$$c_i=(N\mathcal{A}(\chi_1\chi_2\psi_i)|\Psi^{\mathrm{CI}}). \tag{4.5}$$

The absolute value of the norm $|(\Psi^{(1)}|\Psi^{(1)})|$ does then represent a weight of the specific geometrical configuration $(\vec{R}_1,\vec{R}_2)$, which is fully characterized by two distances and one angle β. We put the additional constraint $|\vec{R}_1|=|\vec{R}_2|\equiv R$ on $\Psi^{(1)}$ and located again the dominant configuration in the (R,β) space. In analogy to the discussion above, the associated angular distribution $\widetilde{W}$,

$$\widetilde{W}(\beta)=\int dR\ R^3|(\Psi^{(1)}|\Psi^{(1)})| \tag{4.6}$$

is shown in Fig. 6. Using the $18p$ basis set $\widetilde{W}$ peaks at $\beta=90°$ as expected. For the $7s18p5d$ basis set the maxi-

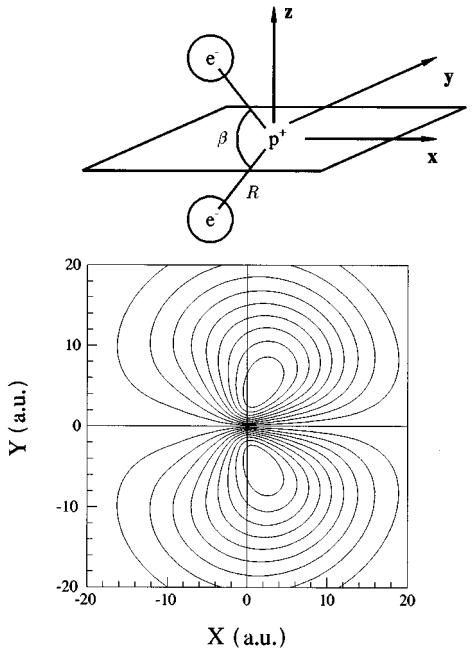

FIG. 7. Schematic representation of the two-particle model function discussed in the text. In addition, the absolute squared value $|(\Psi^{(1)}|\Psi^{(1)})|$ of $\Psi^{(1)}$ is shown for $\beta=108°$ and $R=8.0$ a.u. in the x-y plane. The contour lines are evenly spaced and the ratio between the innermost and outermost line is 5.

mum of $\widetilde{W}$ occurs at $\beta=108°$ for H^{2-} and $\beta=97°$ for He^-. The slightly larger values obtained for β in comparison to $\phi_{\max}$ reflect that only the positions of two electrons have been ''fixed,'' whereas the third one may adapt to their positions. Thus, the optimal angle $\beta_{\max}$ between the two GTOs χ_1 and χ_2 is somewhat larger than $\phi_{\max}$ in the analysis employing $\Psi^{(3)}$ and the distribution over β is much broader than that over ϕ.

In order to plot the resulting one-particle function $\Psi^{(1)}$ the position vectors $\vec{R}_1$ and $\vec{R}_2$ have been defined by the Cartesian coordinates $(x,0,\pm z)$ fixing two electrons in the x-z plane above and below the x-y plane accommodating the proton (Fig. 7). Given this geometrical arrangement the function $\Psi^{(1)}$, which describes the third electron, consists essentially of p_y functions [recall that the CI vector is dominated by $(np_x n'' p_y n'' p_z)$ configurations]. For example, if the $18p$ basis set is used $\Psi^{(1)}$ is an exclusive combination of p_y orbitals, whereas for the $7s18p5d$ basis set there are in addition d_{xy} contributions to $\Psi^{(1)}$. Thus, in this specific one-particle picture one may think of the third electron to occupy a p orbital, which polarizes according to the positions of the other two electrons. This situation is displayed in Fig. 7. Here the absolute value of $\Psi^{(1)}$ is shown; however, both the real and imaginary parts give essentially the same picture. In this representation the nature of the nodal plane mentioned above is quite obvious. The plane defined by the nucleus and any two electrons corresponds to the nodal plane of the polarized p orbital representing the third electron. Thus, in case of the $(2p^3)^4S^o$ state the three electrons and the nucleus can never adopt a truly planar configuration analogous to those of the $AX_3{}^{2-}$ molecular dianions.

V. SUMMARY AND CONCLUSIONS

We have investigated the existence of a resonance state with three electrons and one proton using the complex rotation method in conjunction with the MR-CI approach. From our experience with bound dianions, a state with three equivalent electrons was expected to be a promising candidate, and this criterion is fulfilled for the $(2p^3)^4S^o$ state. In our study we have treated the nuclear charge Z as a parameter, since the $^4S^o$ state of He^- is known to be bound. Starting from this bound $(2p^3)$ state, we have reduced Z and followed the quartet state as it becomes rapidly unbound and moves into the $(2p^2\epsilon p)$ continuum. At $Z\approx1.4$ the $^4S^o$ state becomes even unbound with respect to the $(2p^1)^2P^o$ state, i.e., the channel to the $(2p^1\epsilon p\epsilon' p)$ continuum opens, and the associated width function exhibits a cusp. For $Z=1$ the $(2p^3)$ resonance state shows still a negative energy and the system is thus stable with respect to complete breakup into the nucleus and three free electrons. With our largest basis set the H^{2-} resonance position is then 1.4 eV above the $(2p^2)^3P^e$ state of H^- and the lifetimes is 3.8×10^{-16} s. We note that the resonance state is stabilized, if the basis set is enlarged, i.e., the resonance position is decreased and the lifetime is increased.

From an experimental point of view there seems to be no easy way to observe the H^{2-} resonance state. Since its spin symmetry is a quartet it cannot be seen in the electron scattering cross section of the $^1S^e$ ground state of H^-, which shows indeed no structure [10,11]. Instead, one would have to scatter from the H^- $^3P^e$ state, which is, however, metastable by itself and may radiatively decay via a dipole allowed transition to the $(1s)^1(2p)^1{}^3P^o$ state, which is unstable with respect to electron emission. It may be easier to observe the analogous dianionic state of the boron atom. Apart from the increased nuclear charge, which is counterbalanced by the $1s$ and $2s$ electrons, the B^{2-} $^4S^o$ $(1s)^2(2s)^2(2p)^3$ state perfectly resembles the investigated H^{2-} resonance state. In this case the target in a potential electron scattering experiment is the bound electronic ground state of the B^- anion.

The existence of a metastable H^{2-} state has been rationalized by comparing it with molecular dianions of the $AX_3{}^{2-}$ type and a series of $^4S^o$ (np^3) states of the He^- anion. Furthermore, a system of three equivalent electrons and a nucleus of charge Z was studied in the finite-dimension limit. From the trends observed for these analogous systems the picture of an increased electron-nucleus-electron angle emerged. For a (p^3) electronic configuration one would expect an interelectronic angle of 90°. However, the more diffuse the different species get, the further this angle is opened and tends to a limit of 120°. This limiting value is associated to the classical minimal energy configuration of three equivalent negative charges fixed at a common radial distance from a positively charged center.

We then have substantiated this picture by analyzing the complex wave function of the resonance state itself. Two overlap-with-a-model function analysis schemes were applied. Loosely speaking, on the one hand, the contribution of a certain ammonialike geometrical configuration of the three electrons was considered, and, on the other hand, the probability amplitude of one electron was calculated keeping the

other two electrons at ''fixed'' positions. The first analysis scheme revealed that one may in fact think of the $^4S^o$ states of H^{2-} and He^- in terms of an ammonialike C_{3v} configuration of the electrons, and the associated electron-nucleus-electron angle is indeed opened to 99° for He^- and 104° for H^{2-}. The second scheme exhibited another way to rationalize these stabilizing correlation effects. The three electrons may be thought of as occupying p orbitals that polarize accordingly to the positions of the other electrons. In both cases the same tendencies, which were derived from the comparison with the analog systems mentioned above, have been observed. In going to smaller Z values the $^4S^o$ state gets more diffuse and the configuration gets closer to the 120° limit of the AX_3^{2-} cluster dianions. However, from a symmetry analysis it became clear that this limit cannot be reached, since the plane defined by any two electrons and the nucleus represents a nodal plane for the third electron. Clearly, both of these ways to visualize the H^{2-} resonance state are only caricatures of this highly correlated system. However, they provide means to illuminate the essential physical effects that make the existence of this short-lived state possible.

ACKNOWLEDGMENTS

This work would not have been possible without the help of Bernd Engels and Hans Ulrich Suter who generously put the new version of the MRDCI program to our disposal and helped us to change their code. Computer time has been provided by the Rechenzentrum der Universität Heidelberg. Financial support by the Deutsche Forschungsgemeinschaft is gratefully acknowledged.

[1] D. S. Walton, B. Peart, and K. Dolder, J. Phys. B **3**, L148 (1970).
[2] D. S. Walton, B. Peart, and K. Dolder, J. Phys. B **4**, 1343 (1971).
[3] B. Peart and K. Dolder, J. Phys. B **6**, 1497 (1973).
[4] H. S. Taylor and L. D. Thomas, Phys. Rev. Lett. **28**, 1091 (1972).
[5] L. D. Thomas, J. Phys. B **7**, L97 (1974).
[6] B. Simon, Int. J. Quantum Chem. **14**, 529 (1978).
[7] F. Robicheaux, R. P. Wood, and C. H. Greene, Phys. Rev. A. **49**, 1866 (1994).
[8] C. A. Nicolaides and D. R. Beck, J. Chem. Phys. **66**, 1984 (1977).
[9] C. A. Nicolaides and D. R. Beck, Int. J. Quantum Chem. **14**, 462 (1978).
[10] L. H. Andersen, D. Mathur, H. T. Schmidt, and L. Vejby-Christensen, Phys. Rev. Lett. **74**, 892 (1995).
[11] L. Vejby-Christensen, D. Kella, D. Mathur, H. B. Pedersen, H. T. Schmidt, and L. H. Andersen, Phys. Rev. A **53**, 2371 (1996).
[12] J. M. Levy-Leblond, J. Phys. B **4**, L23 (1971).
[13] E. H. Lieb, Phys. Rev. Lett. **52**, 315 (1984).
[14] C. F. Bunge and A. V. Bunge, Int. J. Quantum Chem. **12**, 345 (1978).
[15] D. R. Beck and C. A. Nicolaides, Chem. Phys. Lett. **59**, 525 (1978).
[16] M. K. Scheller, R. N. Compton, and L. S. Cederbaum, Science **270**, 1160 (1995).
[17] J. Kalcher and A. F. Sax, Chem. Rev. **94**, 2291 (1994).
[18] T. Sommerfeld, U. V. Riss, H.-D. Meyer, and L. S. Cederbaum, Phys. Rev. Lett. **77**, 470 (1996).
[19] J. Aguilar and J. M. Combes, Commun. Math. Phys. **22**, 269 (1971).
[20] E. Balslev and J. M. Combes, Commun. Math. Phys. **22**, 280 (1971).
[21] B. Simon, Commun. Math. Phys. **27**, 1 (1972).
[22] B. Simon, Ann. Math. **97**, 247 (1973).
[23] W. P. Reinhardt, Annu. Rev. Phys. Chem. **33**, 207 (1982).
[24] B. R. Junker, Adv. At. Mol. Phys. **18**, 207 (1982).
[25] N. Moiseyev, P. R. Certain, and F. Weinhold, Mol. Phys. **36**, 1613 (1978).
[26] C. W. McCurdy, in *Autoionization*, edited by A. Temkin (Plenum, New York, 1985).
[27] G. W. F. Drake, Phys. Rev. Lett. **24**, 126 (1970).
[28] B. Engels, H. U. Suter, V. Pless, R. J. Buenker, and S. D. Peyerimhoff (private communications).
[29] H.-D. Meyer and S. Pal, J. Chem. Phys. **91**, 619 (1989).
[30] K. R. Milfeld and N. Moiseyev, Chem. Phys. Lett. **130**, 145 (1986).
[31] E. Haller, H. Köppel, and L. S. Cederbaum, J. Mol. Spectrosc. **111**, 377 (1985).
[32] M. K. Scheller and L. S. Cederbaum, J. Chem. Phys. **99**, 441 (1993).
[33] C. A. Nicolaides, M. Chrysos, and Y. Komninos, Phys. Rev. A **41**, 5244 (1990).
[34] Y. Komninos, M. Chrysos, and C. A. Nicolaides, Phys. Rev. A **38**, 3182 (1988).
[35] J. G. Loeser, J. Chem. Phys. **86**, 5635 (1987).
[36] K. Andersson, M. R. A. Blomberg, M. P. Fülscher, V. Kellö, R. Lindh, P.-A. Malmqvist, J. Noga, J. Olsen, B. O. Roos, A. J. Sadlej, P. E. M. Siegbahn, M. Urban, and P. O. Widmark, MOLCAS Version 3, University of Lund, Sweden, 1994.